

# Adaptive Wide Angle PWM Control Strategy of BLDC Motor Drive for Efficiency Optimization and Wide Speed Control Range

Kai Sheng Kan

Department of Electrical and Control Engineering  
National Chiao Tung Univ.  
Hsinchu, Taiwan  
ken3873329@yahoo.com.tw

Ying-Yu Tzou

Department of Electrical and Control Engineering  
National Chiao Tung Univ.  
Hsinchu, Taiwan  
yytzou@mail.nctu.edu.tw

**Abstract**—To reduce the torque pulsation of BLDC motors caused by conventional 120° conduction control, this paper proposes an adaptive wide angle control scheme with adjustable modulation waveform to achieve wide speed control range with efficiency optimization. The proposed adaptive soft commutation PWM modulation scheme is based on an adjustable modulation waveform with wide angle conduction period (more than 120° but less than 180°) and control the phase current with quasi-sinusoidal waveform to minimize the pulsation torque due to commutation. By using the adaptive PWM modulation scheme, the RMS value of phase current is lower than conventional 120° conduction mode under the same testing condition. Compared with the traditional control method, torque ripple of the BLDC motor can be reduced significantly by using the proposed control method. Simulation and experimental verification have been given to illustrate the performance of the proposed PWM strategy.

**Index Terms**—adaptive wide-angle control, adaptive soft commutation, back-EMF, BLDC motor, torque ripple

## I. INTRODUCTION

BLDC motors with trapezoidal flux distribution have been adopted in various industrial and home appliance applications, because of the high efficiency, high power density, low acoustic noise, easier control and low maintenance cost. An ideal brushless dc motor has a trapezoidal back-EMF waveform and zero torque ripple is produced when the motor is fed by an ideal rectangular current waveform. However, in a practical BLDC motor the back EMF waveform is more similar as a round-off trapezoidal waveform. In this case, the conventional 120° PWM scheme will produce current ripple while commutation [1], and different PWM modulation schemes were developed to reduce torque ripples due to these commutation current ripples [2]-[4]. Even though the fed current can be controlled rectangular by above methods, the torque ripple is still produced due to the non-ideal back-EMF or quasi-sinusoidal back-EMF resulted by non-uniformity and placement of magnetic stators.

To reduce torque ripple for those motors, sinusoidal current drive is better than square drive control. Several papers have proposed a wide angle control method [5]-[9], which make the current waveform quasi-sinusoidal. With this method, it can reduce torque ripple, increase torque constant compared with 120° conduction scheme, and realize sensorless drive scheme with varied active angular period from 120° to about 170°. However, phase current will be delayed compared with its PWM command due to winding dynamics and back EMF. When operating in high speed range, significant phase delay and current waveform distortion will be resulted due to the electrical time constant and back EMF of the motor. In these cases, if the wide angle PWM modulation has not been properly adjusted, higher torque ripples will be resulted compared with the conventional 120° PWM scheme. To solve this problem, this paper presents an adaptive wide angle control method, the PWM modulation waveform is a parametric function of control duties. The proposed scheme can be used for sensorless BLDC drives for efficiency optimization with wide speed control range.

## II. ANALYSIS FOR CONVENTIONAL 120 DEGREE PWM METHOD

Fig. 1 shows the block diagram of the proposed adaptive wide angle PWM control scheme for three-phase BLDC motor. A parametric PWM modulation waveform is defined with three parameters:  $k1 = \theta_{soft}$ ,  $k2 = \text{duty}$ , and  $k3 = \text{full duty} \times X\%$ . In a special case for  $k1 = 0$  and  $k3 = 0$ , it becomes the conventional hard commutation scheme with a 120° conduction angle, Fig. 2 shows its typical switching waveforms at full duty.

In this operation mode, each switch conducts for 120° and there are six step in each periodic cycle. During each commutation interval, only two windings are conducted and the third winding is floating for 60 electrical degrees. The pole voltage  $v_{xo}$  is  $0.5v_{dc}$  ( $x = a, b, c$ ) when upper switch is on, and is  $-0.5v_{dc}$  when lower switch is on, and  $v_{xo}$  is zero when the phase is floating. It needs to mention that in this paper we ignore the influence on the neutral point voltage from back-EMF, that is, we assume  $v_{no} = 0$  in 120° conduction

---

This work was supported by the National Science Council, Taipei, Taiwan, R. O. C. Project no. NSC99-2622-E-009-014-CC1.

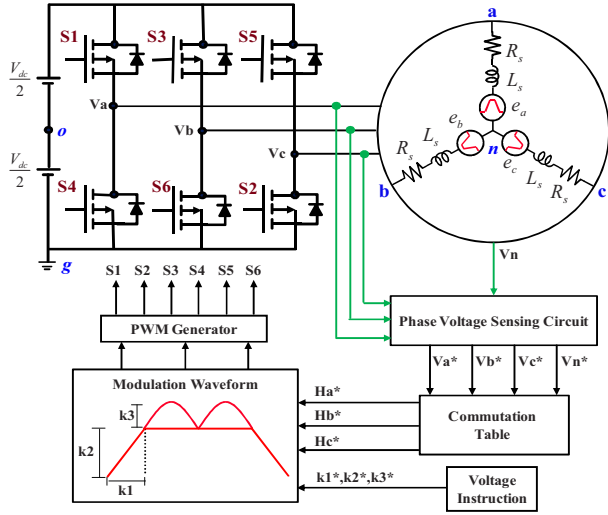


Figure 1. Block diagram of the proposed adaptive wide angle PWM control scheme for three-phase BLDC motor.

mode. The phase voltage can be computed as  $v_{xn} = v_{xo} - v_{no}$ . Assume the electrical time constant is very small compared with the commutation interval and at steady-state the phase current can be presented as:

$$\begin{cases} i_x = I_o & \text{when } v_{xn} = 0.5v_{dc}, \\ i_x = -I_o & \text{when } v_{xn} = -0.5v_{dc}. \end{cases} \quad (1)$$

The phase current of three phase in  $0^\circ \sim 30^\circ$  in Fig. 2 is

$$i_a = I_o, i_b = -I_o, \text{ and } i_c = 0. \quad (2)$$

The waveform of back-EMF is approximate to the experimental fan motor. Therefore, the back-EMF in  $0^\circ \sim 30^\circ$  in Fig. 2 is

$$e_a = \frac{E_m}{60^\circ} \omega t + \frac{E_m}{2}, e_b = -E_m, \text{ and } e_c = \frac{E_m}{2} - \frac{E_m}{60^\circ} \omega t. \quad (3)$$

Then the electrical torque of three phase motor can be calculated as:

$$T_e = \frac{e_a i_a + e_b i_b + e_c i_c}{\omega_m} = \frac{1}{\omega_m} (E_m I_o + \frac{E_m I_o}{60^\circ} \omega t), \quad (4)$$

$$0^\circ \leq \omega t \leq 30^\circ,$$

where  $i_a$ ,  $i_b$ , and  $i_c$  are phase current,  $e_a$ ,  $e_b$ , and  $e_c$  are back-EMF, and  $I_o$ ,  $E_m$  are peak value of phase current and back-EMF, respectively. The  $\omega_m$  is rotor angular speed. Because the torque ripple is symmetric at every 30 electric degree, the average torque value can be calculated as:

$$T_{avg\_120} = \frac{1}{30^\circ} \int_0^{30^\circ} T_e d\omega t = \frac{1.75 E_m I_o}{\omega}. \quad (5)$$

And the peak to peak value of torque is

$$\Delta T_{pp\_120} = T_e(30^\circ) - T_e(0^\circ) = \frac{0.5 E_m I_o}{\omega}. \quad (6)$$

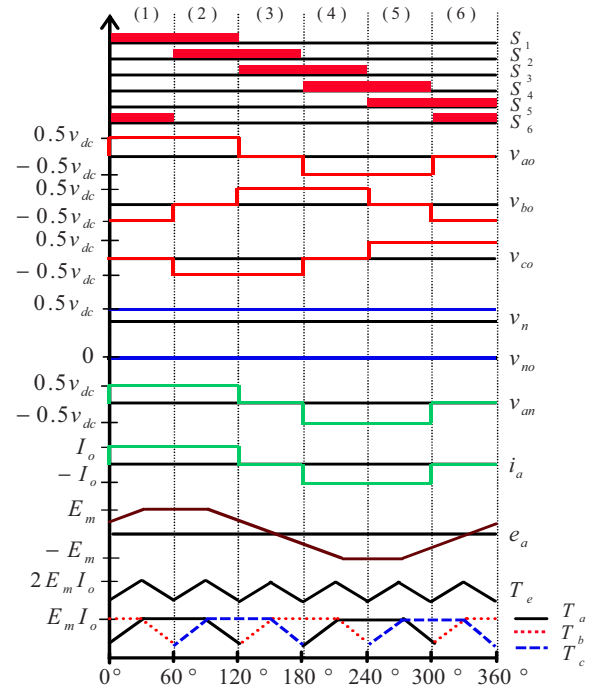


Figure 2. Switching waveforms of 120° conduction mode at full duty.

The percentage of torque ripple is defined as the ratio of the peak-to-peak value to its average value, and the torque ripple factor can be calculated as:

$$T_{rf\_120} = \frac{\Delta T_{pp\_120}}{T_{avg\_120}} \times 100\% = 28.5\%. \quad (7)$$

### III. ANALYSIS FOR WIDE ANGLE QUASI-SINUSOIDAL PWM METHOD

#### A. Wide Angle Mode with Soft Commutation

Fig. 3 shows the waveform of wide angle conduction mode with soft commutation. The concept of soft commutation is to change the PWM duties gradually when crossing the commutation instant. In the beginning and ending period of each excited phase, the switches are controlled to gradually increase and decrease between zero and their target PWM duty. Therefore, the voltage  $v_{xo}$  equals  $0.5v_{dc}$  or  $-0.5v_{dc}$  in normal conduction period just like 120° conduction mode, increases or decreases gradually during its commutation interval.

The key concept of the PWM control scheme is to preserve 120° conduction period, while adding an additional conduction period with soft commutation at the beginning and ending during each commutation interval. The additional soft period can be adjusted according to a defined curve as a function of control duty. Fig. 3 shows operating waveforms at the 150° conduction mode, where the soft commutation degree at two terminals of each excited phase is 15°.

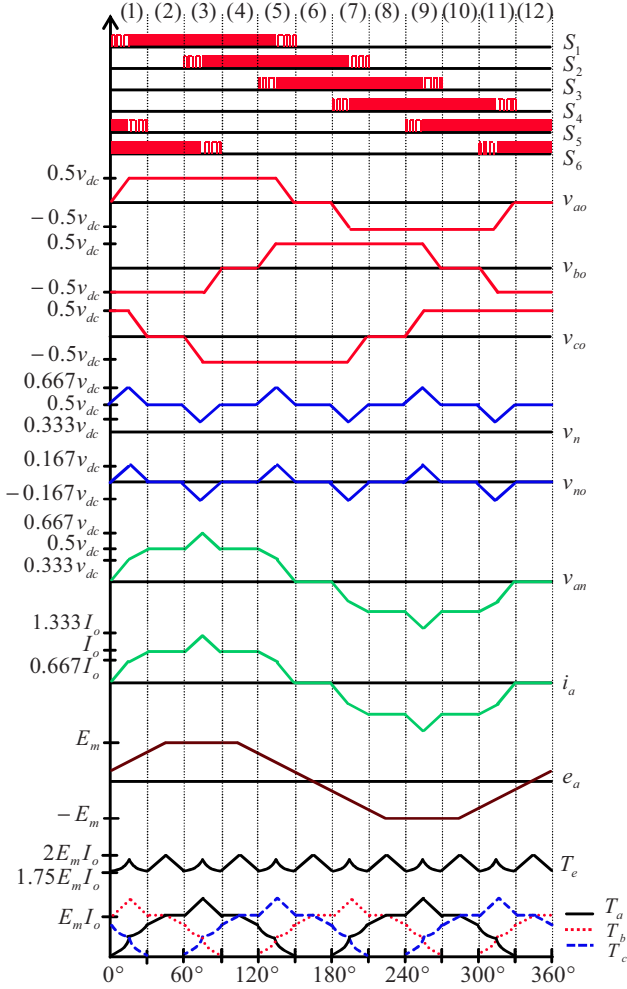


Figure 3. Ideal operation waveforms of wide angle (150°) PWM modulation method with soft commutation.

This mode is a combination of 120° and 180° conduction mode. Three phases conduct at odd step while two phases conduct at even step, each step is 30 electric degrees. At even step the neutral point voltage is just like 120° conduction mode,  $v_n = 0.5v_{dc}$ . Fig. 4 shows the neutral point voltage during odd step, which can be separated into two condition. Fig. 4(a) represents the step (1), first we can derive neutral point voltage without soft commutation as follow:

$$\begin{cases} v_n = v_{dc} - i_a R - L \frac{di_a}{dt} - e_a, \\ v_n = i_b R + L \frac{di_b}{dt} - e_b, \\ v_n = v_{dc} - i_c R - L \frac{di_c}{dt} - e_c. \end{cases} \quad (8)$$

Assume the three phase circuit is balance, the three phase back-EMF and phase current in Fig. 4(a) have the following relation:

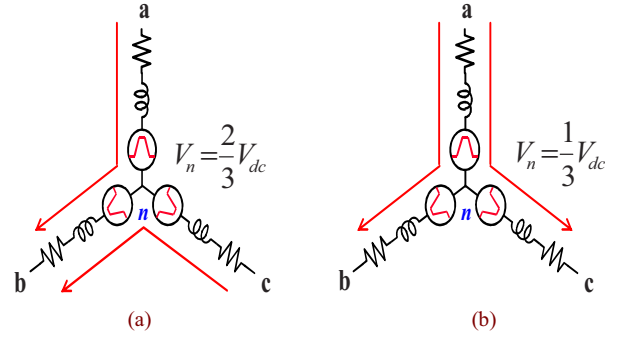


Figure 4. Circuit in different conducting intervals. (a) Two upper and one lower leg switches on. (b) One upper and two lower leg switches on.

$$e_a + e_b + e_c = 0, \quad (9)$$

$$i_a + i_c = i_b. \quad (10)$$

By substituting (9) and (10) into the summation of (8), it is easily shown that  $v_n = 2v_{dc}/3$  at step (1) without soft commutation. Similarly, Fig. 4(b) represents the step (3) where the neutral voltage can be calculated as  $v_{dc}/3$ . Caused by soft commutation, the waveform of neutral point voltage increases to  $2v_{dc}/3$  gradually in  $0^\circ \sim 15^\circ$  while decreases to  $v_{dc}/3$  gradually in  $60^\circ \sim 75^\circ$ .

It can be observed from Fig. 3 that the torque waveform is symmetric at  $0^\circ \sim 15^\circ$  and  $15^\circ \sim 30^\circ$ ,  $30^\circ \sim 45^\circ$  and  $45^\circ \sim 60^\circ$ . The phase current in  $0^\circ \sim 15^\circ$  can be expressed as:

$$\begin{aligned} i_a &= \frac{2I_o/3}{15^\circ} \omega t, \quad i_b = \frac{-I_o/3}{15^\circ} \omega t - I_o, \\ \text{and } i_c &= \frac{-I_o/3}{15^\circ} \omega t + I_o. \end{aligned} \quad (11)$$

The back-EMF for each phases are:

$$e_a = \frac{E_m}{60^\circ} \omega t + \frac{E_m}{4}, \quad e_b = -E_m, \quad \text{and } e_c = \frac{3E_m}{4} - \frac{E_m}{60^\circ} \omega t. \quad (12)$$

The torque in  $0^\circ \sim 15^\circ$  can be obtained from equation (11), (12), and (4):

$$T_{e1} = \frac{1}{\omega_m} \left[ \frac{E_m I_o}{(30^\circ)^2} (\omega t)^2 + \frac{7E_m I_o}{4} \right], \quad 0^\circ \leq \omega t \leq 15^\circ. \quad (13)$$

Similarly, the phase current in  $30^\circ \sim 45^\circ$  are the same as (2), and the back-EMF in  $30^\circ \sim 45^\circ$  are just like (12). Therefore, the torque in  $15^\circ \sim 30^\circ$  can be got:

$$T_{e2} = \frac{1}{\omega_m} \left[ \frac{E_m I_o}{60^\circ} \omega t + \frac{5E_m I_o}{4} \right], \quad 30^\circ \leq \omega t \leq 45^\circ. \quad (14)$$

The total average torque is the combination of  $T_{e1}$  and  $T_{e2}$ , which can be shown as follow:

$$T_{avg\_soft} = \frac{1}{30^\circ} \left( \int_0^{45^\circ} T_{e1} d\omega + \int_{30^\circ}^{45^\circ} T_{e2} d\omega \right) = \frac{1.854 E_m I_o}{\omega}. \quad (15)$$

The peak to peak value of torque is

$$\Delta T_{pp\_soft} = T_{e2}(45^\circ) - T_{e2}(30^\circ) = \frac{0.25 E_m I_o}{\omega}. \quad (16)$$

Therefore the torque ripple can be calculated as :

$$T_{rf\_soft} = \frac{\Delta T_{pp\_soft}}{T_{avg\_soft}} \times 100\% = 13.5\%. \quad (17)$$

Comparing (7) and (17), the torque ripple is reduced from 28.5% to 13.5% by using the proposed wide angle PWM scheme with soft commutation.

### B. Wide Angle Mode with Sin-Wave Injection

Fig. 5 shows the waveforms of wide angle conduction mode with sin-wave injection. The switch waveforms are similar to wide angle mode with soft commutation, so we ignore them here. It is clear that from the waveform of  $v_{xo}$ , the difference between this mode and wide angle mode with soft commutation is that two half-period sin wave is added to the 120° conduction period, where the period cycle of sin wave is equal to 120 electronic degrees of the motor. Therefore, the neutral point voltage is just like a sin wave at even step. Here taking the amplitude of sin is equal  $0.1v_{dc}$  for example, then the neutral voltage can be calculate as follow:

$$v_n = \begin{cases} 0.8v_{dc} \times \frac{2}{3} = 0.533v_{dc} & \text{when } \omega t = 15^\circ, \\ 0.4v_{dc} + 0.1v_{dc} \times \sin \frac{\pi}{4} = 0.471v_{dc} & \text{when } \omega t = 30^\circ, \\ 0.8v_{dc} \times \frac{1}{3} = 0.267v_{dc} & \text{when } \omega t = 45^\circ. \end{cases} \quad (18)$$

Then we can calculate phase current at  $0^\circ \sim 15^\circ$  as:

$$\begin{cases} i_a = \frac{0.676I_o}{15^\circ} \omega t + 0.058I_o, \\ i_b = \frac{-0.26I_o}{15^\circ} \omega t - I_o, \\ i_c = \frac{-0.266I_o}{15^\circ} \omega t + I_o. \end{cases} \quad (19)$$

And the back-EMF are the same as (12). The torque at  $0^\circ \sim 15^\circ$  can be present as:

$$T_{e1} = \frac{1}{\omega_m} \left[ \frac{0.942 E_m I_o}{(30^\circ)^2} (\omega t)^2 - \frac{0.012 E_m I_o}{30^\circ} \omega t + 1.7645 E_m I_o \right], \quad 0^\circ \leq \omega t \leq 15^\circ. \quad (20)$$

The torque at  $30^\circ \sim 45^\circ$  is just equal to (14), then we can also calculate the average torque value as:

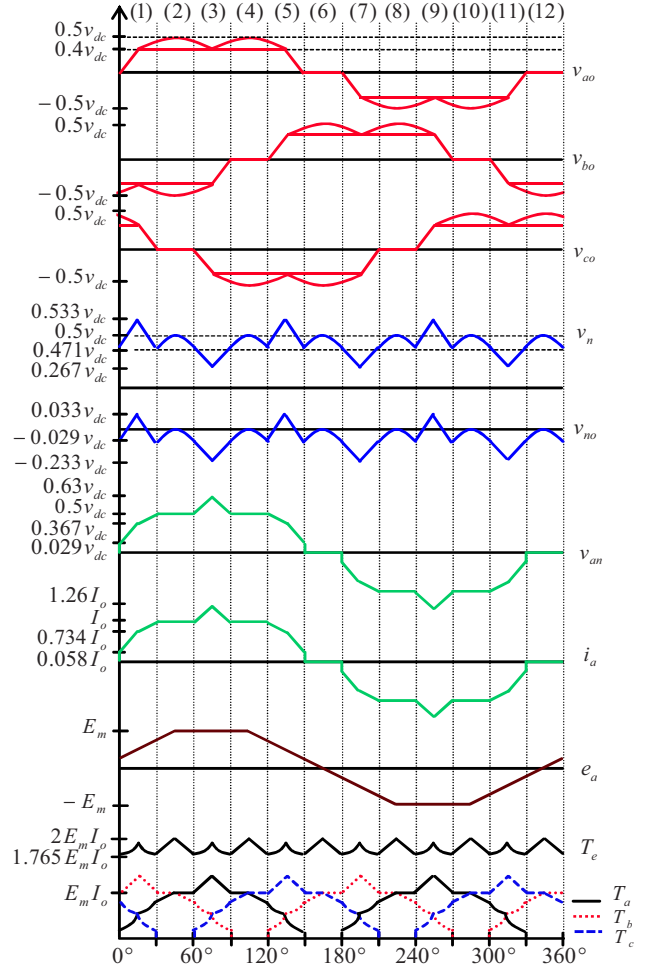


Figure 5. Ideal operation waveform of wide angle PWM modulation method with sin-wave injection.

$$T_{avg\_sin} = \frac{1}{30^\circ} \left( \int_0^{45^\circ} T_{e1} d\omega + \int_{30^\circ}^{45^\circ} T_{e2} d\omega \right) = \frac{1.862 E_m I_o}{\omega}. \quad (21)$$

And the peak to peak value of torque is:

$$\Delta T_{pp\_sin} = \frac{0.235 E_m I_o}{\omega}. \quad (22)$$

Finally, the torque ripple in this mode can be calculate as:

$$T_{rf\_sin} = \frac{\Delta T_{pp\_sin}}{T_{avg\_sin}} \times 100\% = 12.6\%. \quad (23)$$

Comparing (6) and (23), the torque ripple is reduced from 28.5% to 12.6% by the wide angle mode with sin-wave injection.

### C. Analysis of Soft Commutation Degree (k1)

In this section, the appropriate conduction degree of soft commutation will be discussed. It is clear that, to get better

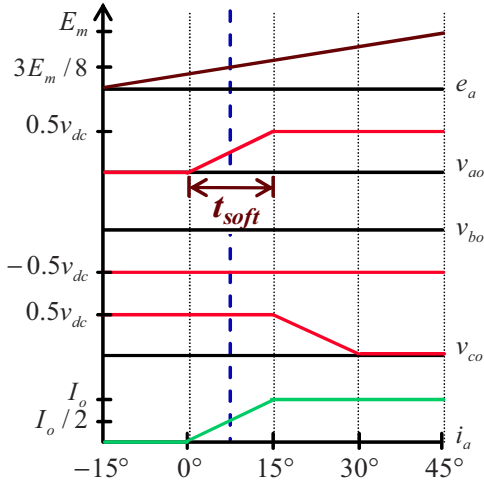


Figure 6. Ideal operation waveform in commutation period.

efficiency of motor at different speed range, the degree of soft commutation will never maintain a constant, it must be a variable which varied with different speed range.

The purpose of soft commutation is making the current waveform smooth. Therefore, in the soft commutation period, the most important thing is that whether the current waveform can reach the voltage command. In other words, we should find out the limited rising slope of current in soft commutation period. If the slope of voltage command is smaller than the limited rising current slope, then the current can always reach the voltage command in commutation. Fig. 6 shows the waveform in commutation period. In  $0^\circ \sim 15^\circ$ , it is like the step (1) in Fig. 3, therefore we can calculate the slope of current from (8) as :

$$\frac{di_a}{dt} = \frac{v_{dc} - v_n - i_a R - e_a}{L}. \quad (24)$$

When motor operates in high speed range, the larger value of back-EMF, the smaller current slope, or the larger soft commutation time. Here, we make some assumption: the soft commutation degree is  $15^\circ$ , and it is large enough that the current can reach the voltage command. If we take care of PWM-ON time in the middle of soft commutation (at  $7.5^\circ$  in Fig. 6), the value of  $v_n$  is  $2v_{dc}/3$ ,  $e_a$  is  $3E_m/8$  and  $i_a$  is  $I_o/2$ . Then (24) can be present as:

$$\frac{di_a}{dt} = \frac{\frac{v_{dc}}{3} - \frac{I_o}{2}R - \frac{3E_m}{8}}{L}. \quad (25)$$

And the soft commutation time can be calculated as:

$$t_{soft} = \frac{I_o}{di_a/dt}. \quad (26)$$

TABLE I. FAN MOTOR PARAMETERS

Symbol	Quantity	Data
$V_{dc}$	input voltage	12V
$f_{sw}$	switching frequency	20KHz
$P$	poles of motor	4poles
$L_s$	stator winding inductance	0.22mH
$R_s$	stator winding resistance	$2.3\Omega$
$K_E$	back-EMF constant (peak line-to-line)	0.54mV/rpm
$J_m$	moment inertia	$0.1\mu\text{kg} \cdot \text{m}^2$

TABLE II. CALCULATED SOFT COMMUTATION DEGREE

Duty	20%	30%	40%	50%	60%	70%	80%	90%
$\theta_{soft} (k1)$	$0.16^\circ$	$0.41^\circ$	$0.89^\circ$	$1.95^\circ$	$3.37^\circ$	$6.13^\circ$	$8.95^\circ$	$14.64^\circ$

From (25) and (26), we can calculate the appropriate soft commutation degree at an certain speed.

## VI. SIMULATION AND EXPERIMENT RESULTS

In this section, some simulation and experimental results are provided to evaluate the performances of novel control method, where the simulation platform is based on PSIM. In the simulation and experiments, we let upper switch work as “PWM” and the lower switch work as “always on”. Table I shows the fan motor parameters.

Fig. 7 shows the simulation waveform of phase current and torque at 6000 RPM by different modulation method. Fig. 7(a) is the waveform of  $120^\circ$  conduction mode, Fig. 7(b) is wide angle conduction mode with soft commutation, Fig. 7(c) is wide angle conduction mode with sin-wave injection. The RMS value of torque is reduced from 0.348 mN-m to 0.295 mN-m, and the RMS value of phase current is improved from 63.6 mA to 54 mA.

The experiment results are shown in Fig. 8. Fig. 8(a) shows the phase current waveform by conditional  $120^\circ$  conduction mode, Fig. 8(b) shows the phase current waveform by wide angle conduction mode with soft commutation, and Fig. 8(c) shows the phase current by wide angle mode with sin-wave injection. The RMS value of phase current is reduced from 89.9 mA to 84.4 mA at the same speed. Also, the peak-to-peak value has been improved from 528 mA to 506 mA.

Table II is the calculated degree of soft commutation at different duty cycle by above mentioned method. Fig. 9 plots a chart of Table II. Fig. 10 shows the simulation result of form factor with different soft commutation degree at different duty cycle. The horizontal line is the soft commutation degree while the vertical line is the value of form factor.



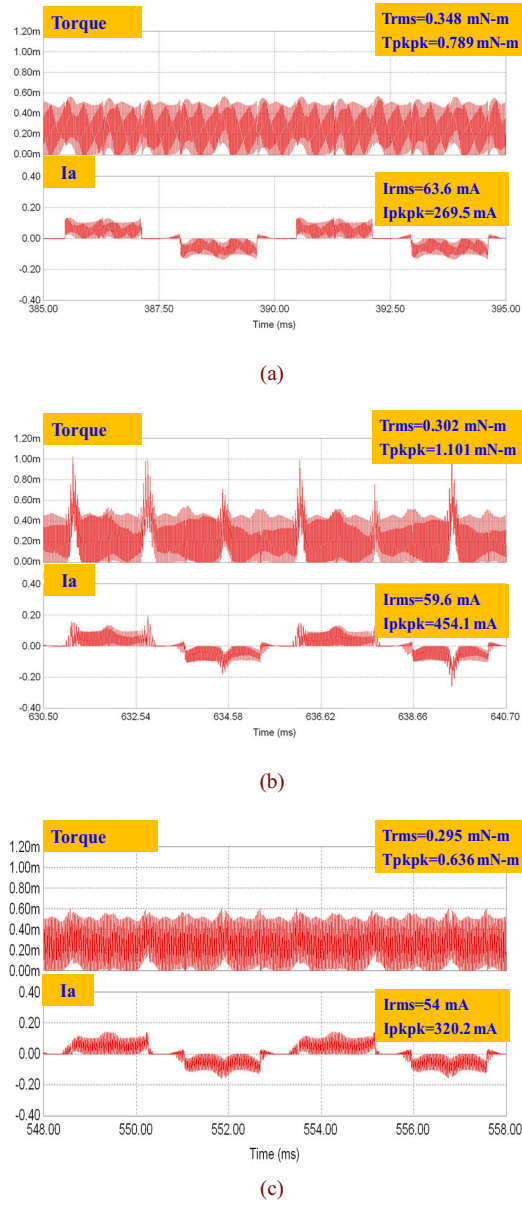


Figure 7. Simulation results of phase current and torque. (a) 120° conduction mode ( $k_1=0^\circ$  &  $k_3=0$ ). (b) wide angle conduction mode with soft commutation ( $k_1=15^\circ$  &  $k_3=0$ ). (c) wide angle conduction mode with sin-wave injection ( $k_1=15^\circ$  &  $k_3=10\%$ ).

Form factor is originally defined as  $I_{rms}/I_{avg}$ , but we know that the torque is produced by the interaction of armature current and a constant  $k_T$ . The torque form factor  $T_{rms}/T_{avg}$  can be used as a measure of efficiency.

When duty is smaller than 50%, the calculated degree is so small that the effect of soft commutation is not apparent. And from Fig. 10(a) we can find that the needed soft commutation degree is smaller than  $5^\circ$ . But when duty is bigger than 50%, the form factor has been improved apparently at the calculated degree. When duty=60% and 70%, the form factor is reduced around  $5^\circ$ , and is reduced

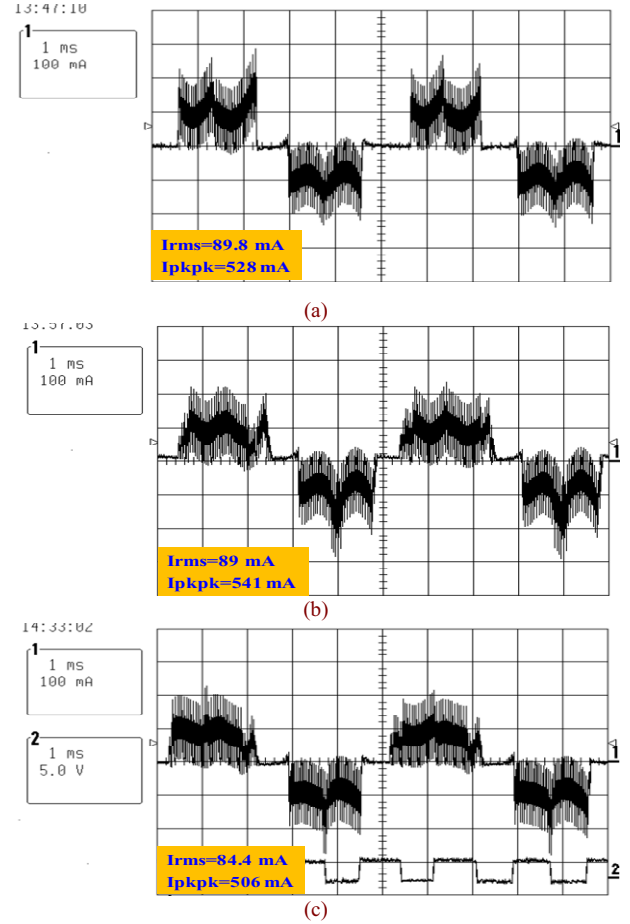


Figure 8. Experiment results of phase current. (a) 120° conduction mode ( $k_1=0^\circ$  &  $k_3=0$ ). (b) wide angle conduction mode with soft commutation ( $k_1=15^\circ$  &  $k_3=0$ ). (c) wide angle conduction mode with sin-wave injection ( $k_1=15^\circ$  &  $k_3=10\%$ ).

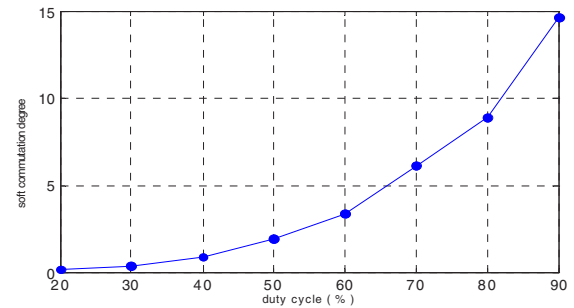


Figure 9. The calculated soft commutation degree at different duty cycle.

around  $10^\circ$  at duty=80% and 90%. Which verify that we can predict an appropriate soft commutation degree at a certain speed.

Fig. 11 is the experimental data curve of variable speed along with RMS value of phase current and peak-to-peak value of phase current by different control method. LV8805 is the commercially available fan motor control IC. It is clear that the novel control method has the smaller RMS and

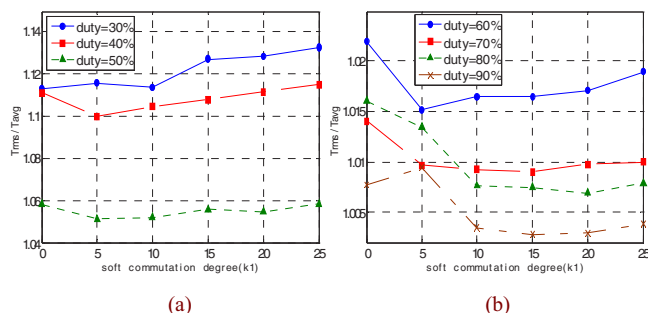


Figure 10. The curve of form factor with different soft commutation degree by simulation. (a) duty cycle=30%~50%. (b) duty cycle=60%~90%.

peak-to-peak value of phase current than 120° conduction mode and commercially available fan motor control IC at the same condition.

From the waveform and the measured value by simulation and experiment, it is clear that the proposed control method can achieve smaller torque RMS and current RMS value at the same operating condition, which implies it also has better efficiency at the same condition.

## V. CONCLUSION

To solve the problem of torque ripple caused by conventional 120° control scheme and current distortion at high speed range caused by wide angle control method. This paper proposes a novel wide angle conduction mode with adjustable modulation waveform. The parameter ( $k_1 \sim k_3$ ) can be adjusted to determine the better modulation waveform at different speed. Therefore, it is possible to obtain a better efficiency if the modulation waveform is adjusted appropriately. By using the adaptive PWM modulation scheme, the RMS value of phase current and torque ripple of the BLDC motor can be reduced significantly under the same testing condition. Simulation and experimental verification have been given to illustrate the performance of the proposed novel control strategy.

## REFERENCES

- [1] R. Carlson, L. M. Michel, and J. C. D. S. Fagundes, "Analysis of torque ripple due to phase commutation in brushless DC machines," *IEEE Trans. Ind. Appl.*, vol. 28, no. 3, pp. 632-638, May/Jun. 1992.
- [2] Y. Liu, Z. Q. Zhu and D. Howe, "Commutation torque ripple minimization in direct torque controlled PM brushless DC drives," in *Proc. IEEE ISA Conf. Rec.*, pp. 1642-1648, 2006.
- [3] S. S. Bharatkar, R. Yanamshetti, D. Chatterjee, and A. K. Ganguli, "Commutation torque ripple analysis and reduction through hybrid switching for BLDC motor drive," in *Proc. IEEE ICIINFS Conf. Rec.*, 2008.
- [4] G. Meng, H. Xiong, and H. Li, "Commutation torque ripple reduction in BLDC motor using PWM\_ON\_PWM mode," in *Proc. IEEE ICEMS Conf. Rec.*, 2009, pp. 1-6.
- [5] C. H. Wu, G. C. Chen, and C. B. Sun, "A wide-angle wave control method of reducing torque ripple for brushless DC motor," *Journal of Shanghai University*, vol. 13, no. 3, 2007, pp. 300-303.
- [6] H. C. Chen, C. K. Hung, and T. Y. Tsai, "BDCM sensorless control for twelve-step square-wave PWM," in *Proc. IEEE PEDS Conf. Rec.*,

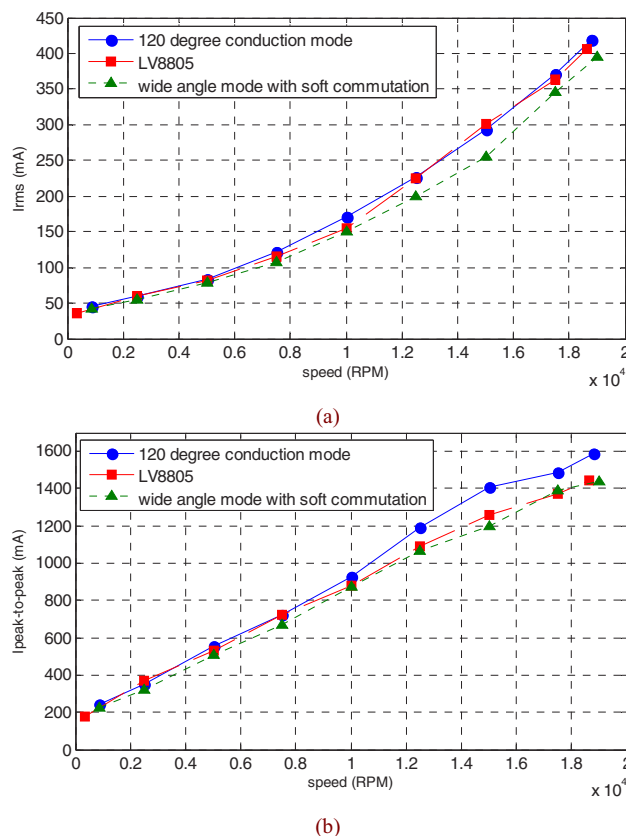


Figure 11. The curve of experimental data. (a) The RMS value of phase current along with variable speed. (b) The peak-to-peak value of phase current along with variable speed.

2009, pp. 511-516.

- [7] C. M. Wang, S. J. Wang, S. K. Lin, and H. Y. Lin, "A novel twelve-step sensorless drive scheme for a brushless DC motor," *IEEE Trans. Magnetics.*, vol. 43, no. 6, pp. 2555-2557, June 2007.
- [8] S. Saha, T. Tazawa, T. Iijima, K. Narazaki, H. Murakami, and Y. Honda, "A novel sensorless control drive for an interior permanent magnet motor," in *Proc. of IECON Conf. Rec.*, pp. 1655-1660. 10011-10011, 2001.
- [9] M. H. Saied, M. Z. Mostafa, T. M. Abdel-Moneim, and H. A. Yousef, "On three-phase six-switch voltage source inverter: a 150-degree conduction mode," in *Proc. of ISIE Conf. Rec.*, pp. 1504-1509, 2006.